JOURNAL

OF THE AMERICAN CHEMICAL SOCIETY

VOLUME 108, NUMBER 6 MARCH 19, 1986

NMR Spectra of Porphyrins. 28.[1] Detailed Solution Structure of a Bacteriochlorophyllide *d* Dimer

Kevin M. Smith,*[2] Frank W. Bobe,[2] Dane A. Goff,[2] and Raymond J. Abraham*[3]

Contribution from the Department of Chemistry, University of California, Davis, California 95616, and The Robert Robinson Laboratories, University of Liverpool, Liverpool L69 3BX, England. *Received July 29, 1985*

Abstract: Methyl bacteriochlorophyllide *d* [Et, Et] in chloroform solution forms a stable dimer which has a sufficiently long lifetime that separate NMR signals are observed from the spectroscopically nonequivalent components of the dimer. The stable dimeric struture is broken down by addition of competitive ligands such as pyridine or methanol. Extensive titration experiments (with methanol-d_4), saturation transfer and nuclear Overhauser enhancement difference experiments at 500 MHz, and specific deuterium labeling of the C-10 and -5a methylenes and of the C-7 propionic side chain enable a complete assignment of the dimer spectrum. The resulting large set of complexation shifts ($\delta_{dimer} - \delta_{monomer}$) allows a precise characterization of the dimer structure with a previously described ring-current model. Two possible structures are shown to be computationally compatible with the observed shifts. One model is a face-to-face structure, whereas the other has a "piggy-back" arrangement of the two molecules. In both structures the separation of the chlorin molecules is ca. 3.5 Å, and the hydroxyl of the C-2 1-hydroxyethyl substituent is coordinated with the magnesium atom of the adjacent molecule in the dimeric pair. Detailed analysis of the observed complexation shifts of the side-chain protons permits a possible differentiation in favor of the piggy-back structure in which an internal hydrogen bond may exist between one of the coordinating hydroxyl groups and the carbonyl of the companion C-7 propionate. Both of the proposed structures bear similarities to the X-ray defined reaction center special pair in *Rhodopseudomonas viridis*, but significant differences are also apparent and are discussed. Finally, a similar dimer is also shown to exist in the bacteriochlorophyll *c* series.

Photosynthetic bacteria are one of a small group of living organisms that possess the ability of plants to harvest and utilize light energy for chemical synthesis,[4] and there has been considerable interest in both the chemistry and physical organization of the photosynthetic contributors in these bacteria.

The bacteriochlorophylls *c*, *d*, and *e* (BChls-*c*, -*d*, -*e*) differ appreciably from the ubiquitous chlorophyll *a* (Chl-*a*) and Chl-*b*. The C-2 vinyl in Chl-*a* and Chl-*b* is replaced with a 1-hydroxyethyl, and the 3-formyl group of Chl-*b* is present in the BChl-*e*, but, again, the Chl-*b* 2-vinyl is replaced with a 1-hydroxyethyl in BChl-*e*. The structures and variety of the BChl-*c*,[5] BChl-*d*,[6] and BChl-*e*[7] are still the subject of active investigation. Some of the earlier confusion regarding the structures of some of the six BChl-*c* homologues was solved when some isomeric pairs of pigments were shown[5] to be diastereomeric owing to *R* and *S* absolute stereochemistry at the 2-(1-hydroxyethyl) substituent, and the chirality of this group was also shown to be important in the BChl-*d*.[6] The rationale behind the various homologous variations in the 4-substituents (ethyl, *n*-propyl, isobutyl, neopentyl) and 5-substituents (methyl or ethyl) and the presence of a meso methyl group in the BChls-*c* and -*e* seem to be associated with the need for the bacteria to tailor their light harvesting (antenna) system to match the specific conditions of their growth environment.[8]

The molecular organization of the reaction center is also known to differ in bacteria and plants. In the reaction center protein of purple photosynthetic bacteria a BChl-*a* dimer serves as the primary donor, while a bacteriopheophytin *a* molecule functions as the first acceptor that remains reduced on a nanosecond time scale.[9] The photoreaction center in plants is considerably more complex.[10] Furthermore, whereas the majority of models proposed to account for the coordination/aggregation tendencies in Chl-*a* have invoked either direct or hydrogen bonded nucleophilic interactions between the central magnesium atom and the 9-keto

(1) Part 27: Smith, K. M.; Goff, D. A.; Abraham, R. J. *Org. Magn. Reson.* **1985**, *22*, 779–783.
(2) University of California.
(3) University of Liverpool.
(4) Allen, M. B. In "The Chlorophylls"; Vernon, L. P.; Seely, G. R., Eds.; Academic Press: New York,; 1966. Holt, A. S. In "The Chemistry and Biochemistry of Plant Pigments"; Goodwin, T. W., Ed.; Academic Press: New York, 1965; pp 3–28.
(5) Smith, K. M.; Kehres, L. A.; Tabba, H. D. *J. Am. Chem. Soc.* **1980**, *102*, 7149–7151. Smith, K. M.; Craig, G. W.; Kehres, L. A.; Pfennig, N. *J. Chromatog.* **1983**, *281*, 209–223.
(6) Smith, K. M.; Goff, D. A. *J. Chem. Soc., Perkin Trans. 1* **1985**, 1099–1115. Smith, K. M.; Goff, D. A.; Barkigia, K. M.; Fajer, J. *J. Am. Chem. Soc.* **1982**, *104*, 3747–3749. Smith, K. M.; Goff, D. A.; Barkigia, K. M.; Fajer, J. *J. Am. Chem. Soc.* **1983**, *105*, 1674–1676.
(7) Brockmann, H., Jr. *Philos. Trans. R. Soc. London, B* **1976**, *273*, 277–285. Brockmann, H., Jr.; Gloe, A.; Risch, N.; Trowitzsch, W. *Liebigs Ann. Chem.* **1976**, 566–577.
(8) Bobe, F. W. Dissertation, University of California, Davis, CA, 1985.
(9) Overfield, R. E.; Scherz, A.; Kaufmann, K. J.; Wasielewski, M. R. *J. Am. Chem. Soc.* **1983**, *105*, 4256–4260.
(10) Fajer, J.; Fujita, I.; Davis, M. S.; Forman, A.; Hanson, L. K.; Smith, K. M. *Adv. Chem. Ser.* **1982**, *No. 201*, 489–513.

0002-7863/86/1508-1111$01.50/0

and/or 10-carbomethoxy group in ring E,[11,12] the BChls-*c*, -*d*, and -*e* exhibit large red shifts in hexane, and its was suggested that these aggregates could provide viable in vitro models for the antenna array in green and brown photosynthetic bacteria.[13]

In principle, NMR spectroscopy can provide detailed information on the structures of porphyrin and chlorophyll aggregates,[11,14] and as part of a continuing investigation into the solution structures of these aggregates, we have developed a ring-current model of the porphyrin and chlorin rings[15,16] and applied it, with some success, to a variety of complexation studies.[12,17] Here we present the results of a similar NMR investigation into the complexation in solution of methyl 4-ethyl-5-ethylbacteriochlorophyllide *d*, (BChlide-*d* [Et, Et]; **1**).[18]

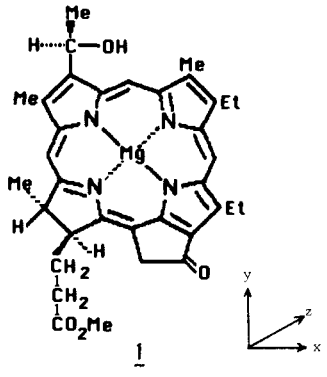

1

In all previous studies of chlorophyll and porphyrin aggregation, the exchange rate between monomer and aggregate and between the different molecules in the aggregate has been fast on the NMR time scale, and therefore only one time-averaged NMR spectrum was observed.[19] However, in the BChlide-*d* studied here, the complexation interaction is sufficiently strong that the molecules in the aggregate are in the slow-exchange limit and two distinct spectra are observed. This unique phenomenon immediately shows that there are two separate sites in the aggregate (and this, in turn, is strong evidence for a dimer structure[20]), and thus that the dimer structure cannot have C_2 symmetry. The extra information present in the spectrum provides an opportunity for obtaining a much more precise structure of this dimer than was possible heretofore. We show here how this complex spectrum can be unravelled and assigned by detailed titration, saturation transfer, integration, and nuclear Overhauser enhancement (NOE) experiments at 500 MHz on unlabeled and regioselectivity deuterated samples of **1**. Subsequently, excess shifts in the dimer were used to provide detailed geometrical parameters.[21]

Theory

The ring-current model used here is that described and parameterized in ref 16, in which the values of the equivalent dipoles required to simulate the ring current of the chlorophyll ring are given together with the close-range approximation used as the network model begins to break down at distances <3.6 Å above the ring. In this approximation the ring-current shifts within a radius of 3.4 Å and half-height 3.6 Å are calculated from the equivalent dipole shifts at the cylinder face by an expression that gives both first- and second-order continuity at the cylinder faces but a discontinuity at the sides of the cylinder, which is precisely where the current loop is situated. The model may be used with some confidence in the aggregation studies, but where the ring-current effect of the Bchlide-*d* on its own side chains is considerable, the discontinuity at the cylinder sides needs to be noted (see later).

As in previous applications of the model to aggregation studies, we restrict the calculations to consideration of a dimer structure in which the planes of the macrocycles are parallel. This is, of course, a convenient and generally accepted premise but nevertheless an arbitrary one. The previous program thus calculated the effect of the ring current of one BChlide-*d* on the other, reversed the process, and compared the average calculated shifts of both molecules in the dimer directly with the observed aggregate shifts. In this case the program was modified so that the calculated ring-current shifts of both molecules in the dimer could be compared directly with the observed shifts by means of the usual least mean squares procedure. The assignment of each of the two resonances of any given proton is thus decided on the basis of the best agreement with the calculated shifts.

The dimer shifts for the face-to-face dimer were calculated explicitly by a variation of the previous procedure, as follows. The "base" macrocycle, i.e., the porphyrin ring from which the ring-current shift is calculated, is fixed in the coordinate system in the xy plane, with the z axis being the fourfold symmetry axis of the porphyrin (given in structure **1**). Consider this as molecule A and the other molecule in the dimer, with center at x, y, z, and rotated θ about the z axis, molecule B. The calculation of the shifts of B due to the ring current of A is straightforward, giving both the shifts and the coordinate array (P_B). It is now necessary to transform the coordinate array to calculate the shifts of A due to the ring current of B. This is done by the successive operations of (a) translate $(-x, -y, -z)$, (b) rotate θ (this converts molecule B to the origin), (c) translate $(-x, -y, -z)$, (d) rotate θ. Now the coordinate array is for molecule A with molecule B at the origin, and the shifts of A due to B can be calculated.

In this calculation the two molecules A and B in the dimer remain the same way up; i.e, this is the calculation for the "piggy-back" model. For the case of the general face-to-face dimer, an amended procedure is used. Molecule B is rotated 180° about the x axis with molecule A unchanged. This is easily achieved with the z matrix input. The molecules are now face-to-face, and the calculation of the shifts (δ_B) and coordinate array (P_B) is as before. To calculate the shifts of A from B, the operations on P_B are (a) translate $(-x, -y, -z)$, (b) rotate θ (molecule B is now at the origin, but inverted relative to A, (c) translate to $(-x, y, z)$, (d) rotate $(-\theta)$. The sign difference of the x translation and rotation compared with the previous calculation compensates for the original rotation about the x axis.

The result is identical for both cases in that a set of calculated shifts for the two molecules in the dimer are produced as functions of the geometrical variables scanned, i.e., the position of molecule B with respect to A (x, y, z) and the rotation of B about the z axis (θ). These calculated shifts can be compared computationally with the observed shifts and the scanning process continued until the best agreement is reached.

(11) (a) Katz, J. J.; Shipman, L. L.; Cotton, T. M.; Janson, J. R. In "The Porphyrins"; Dolphin, D., Ed., Academic Press: New York, 1978; Vol. 5, pp 402–458. (b) Fong, F. K.; Koester, V. J. *J. Am. Chem. Soc.* **1975**, *97*, 6888–6890. (c) Houssier, C.; Sauer, K. *J. Am. Chem. Soc.* **1970**, *92*, 779–791. (d) Kooymann, R. P. H.; Schaafsma, T. J. *J. Am. Chem. Soc.* **1984**, *106*, 551–557.

(12) Abraham, R. J.; Smith, K. M. *J. Am. Chem. Soc.* **1983**, *105*, 5734–5741.

(13) Smith, K. M.; Kehres, L. A.; Fajer, J. *J. Am. Chem. Soc.* **1983**, *105*, 1387–1389.

(14) Katz, J. J.; Brown, C. E. *Bull. Magn. Reson.* **1983**, *5*, 3–49.

(15) Abraham, R. J.; Bedford, G. R.; McNeillie, D.; Wright, B. *Org. Magn. Reson.* **1980**, *14*, 418–425.

(16) Abraham, R. J.; Smith, K. M.; Goff, D. A.; Lai, J.-J. *J. Am. Chem. Soc.* **1982**, *104*, 4332–4337.

(17) Abraham, R. J.; Bedford, G. R.; Wright, B. *Org. Magn. Reson.* **1983**, *21*, 637–642.

(18) The [Et, Et] nomenclature refers, within the homologous series of BChls-*c*, -*d*, and -*e*, to the substituents at the 4- and 5-positions, respectively.

(19) Katz and Brown[14] describe the variable-temperature spectrum of pyrochlorophyll *a* which is in the fast-exchange limit at room temperature but broadens and splits to give multiple resonances below −35 °C; no further details were given.

(20) Note that in a layered aggregate, ring-current effects are such that a molecule inside the sandwich will have very different chemcial shifts from an end molecule (see ref 12 for a full discussion). Simple symmetry arguments alone show that there are only three aggregates that will reproduce the observed spectrum. These are the dimer (AB), a tetramer (ABBA), and a polymer $[(AB)_n]$ in which "n" is so large that end units are not observed (i.e., "n" > 10). Of these, the dimer (which we favor), has a simple chemical interpretation, the tetramer requires two different types of chlorophyll/chlorophyll interaction, and the polymer would give broad unresolved peaks (see ref 11a, Figure 9c) *and* is excluded on the basis of the optical spectra.[13]

(21) Part of this work has appeared as a preliminary communication: Abraham, R. J.; Smith, K. M.; Goff, D. A.; Bobe, F. W. *J. Am. Chem. Soc.* **1985**, *107*, 1085–1087.

Table I. Proton Chemical Shifts (δ) of Methyl Bacteriochlorophyllide *d* [Et, Et] (**1**)

proton	monomer *a*	monomer *b*	monomer *c*	dimer[d]
meso β	9.59	9.53	9.63	9.68 (2)
meso α	9.50	9.35[e]	9.57	6.75, 7.47
meso δ	8.24	8.23	8.40	8.37, 7.91
2a-H	6.33	6.17[e]	6.28	2.54[f]
10-CH_2	5.16	5.18	5.13	5.35, 5.08
	5.02	5.06	4.99	4.89 (2)
8-H	4.39	4.43	4.55	4.67 (2)
7-H	4.16	4.24	4.30	4.63, 4.37
5a-CH_2	4.10	4.03	4.03	4.14, 3.87
4a-CH_2	3.74	3.76	3.78	4.00, 3.97
7d-OMe	3.56	3.45	3.56	3.50, 2.94
3-Me	3.23	3.25	3.25	3.42, 3.13
1-Me	3.29	3.22	3.29	1.19, 1.92
7a-CH_2	2.3–2.5	2.2–2.5	2.3–2.6	2.80, 2.94
7b-CH_2				3.18, 3.40
2b-Me	2.11	2.05	2.03	0.74, 0.41
5b-Me	1.96	1.91	1.89	1.92, 1.92[f]
8-Me	1.70	1.76	1.79	1.42, 2.04[f]
4b-Me	1.70	1.71	1.70	1.68, 2.54[f]

[a] 2.9 mM in $CDCl_3$ + 50 μL of pyridine-d_5. [b] 4.7 mM in $CDCl_3$ + 20 μL of methanol-d_4. [c] 4.6 mM in acetone-d_6 + 45 μL of methanol-d_4. [d] 3.3 mM in $CDCl_3$. [e] Broad signals. [f] Provisional assignments, see text.

Results

The 500-MHz ^1H spectrum of BChlide-*d* [Et, Et] (**1**) monomer, obtained by addition of excess methanol-d_4 or pyridine-d_5 to a solution in $CDCl_3$ or by observing the spectrum in a disaggregating solvent such as acetone-d_6, is first order, apart from the complex multiplet due to the methylene protons of the C-7 side chain. Assignment of the spectrum was made by analogy with related molecules and, where necessary, by decoupling experiments. The latter confirmed the assignment of the C-2b methyl (from H-2a), that of H-8 (from the C-8 methyl), and of the connectivity between the C-4 and C-5 methylene and methyl groups. The assignment of the C-5 side chain to the lower field resonances stems from its proximity to the deshielding C-9 carbonyl group. Assignment of the important β-methyl signals was accomplished by NOE experiments as detectable NOEs to a neighboring (assigned) meso proton are observed upon irradiation of β-methyl signals.

The full assignments and chemical shifts are given in Table I. Note that there is some variation in the chemical shifts in the different solution used. Small intrinsic solvent shifts would be expected in the region of the polar substituents. In the $CDCl_3$ plus methanol-d_4 solution (even with the presence of 20 μL of pure methanol-d_4, a 200-fold excess), the two resonances that show the largest complexation shifts, namely the α-meso and C-2a protons, are still broad due to incomplete dissociation of the dimer and therefore are still offset from the pure dimer shift. This was also the case in the acetone-d_6 solution, illustrating again the considerable stability of the BChlide-*d* dimer. However, addition of a small amount of methanol-d_4 to this solution produced the sharp lines characteristic of the monomer spectrum; these data are recorded in Table I and will be used to obtain the complexation shifts ($\delta_{dimer} - \delta_{monomer}$).

The corresponding spectrum of **1** in pure $CDCl_3$ is shown in Figure 1A, with the low-field spectrum of the meso protons in Figure 2A. The formidable problem of assigning this complex spectrum (Figure 1A) was originally tackled by detailed titration experiments, adding small aliquots of methanol-d_4 (or pyridine-d_5) to the chloroform solution and continuously monitoring the spectrum. In this process the peaks broaden, coalesce, and finally merge into the simple spectrum of the monomer (Figure 2E). Our interpretation of these spectra is that the methanol is breaking down the dimer struture by competitive coordination of the magnesium atom. Thus, the spectrum changes from that of a system in the slow-exchange limit (Figures 1A and 2A), to the broad lines characteristic of intermediate rates of exchange (Figure 2, parts C and D), to finally the sharp simple monomer spectrum (Figure 2E).

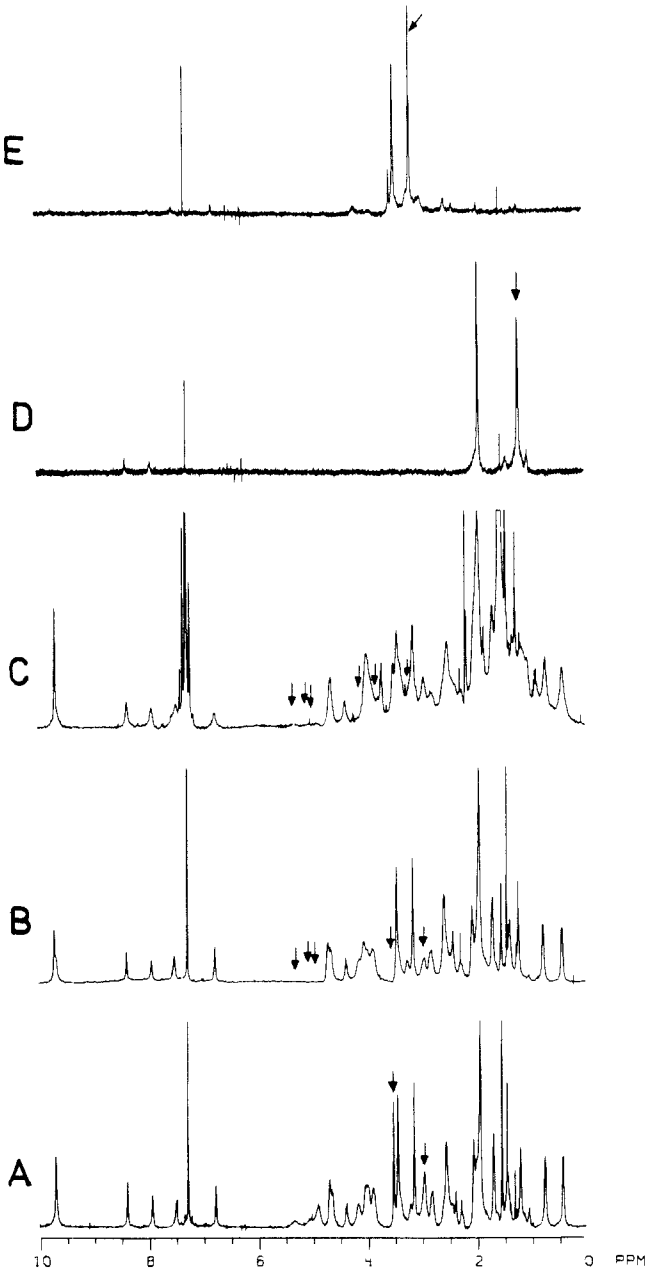

Figure 1. 500-MHz proton NMR spectrum of BChlide-*d* [Et, Et] (**1**): (A) ca. 3 mM in $CDCl_3$, arrows indicate the methyl ester resonances (see text) (for an enlarged version of this spectrum with annotated assignments, see ref 21); (B) the corresponding spectrum of d_5-BChlide-*d* [Et, Et] (**2**), arrows indicate reduced intensities due to deuteration; (C) the spectrum of d_6-BChlide-d [Et, Et] (**5**), arrows indicate reduced intensities due to deuteration; (D) as in A, a combined saturation transfer and NOE experiment irradiating at 1.2 ppm (arrowed); (E) as in D, irradiating at 3.1 ppm (arrowed).

It is possible to assign the meso proton peaks in the dimer from these titration experiments (Table II), but only provisional assignments of most of the remaining dimer spectrum could be made. However, a good indication of the average complexation shift of any peak can be obtained from a plot of the slope of the chemical shift vs. addition of methanol-d_4 in the fast-exchange limit. These plots showed clearly (cf. Table II) the large complexation shifts of the C-1 and C-2 substituents, the much smaller shifts of the C-3 and C-4 substituents, and the very small shifts of the substituents on the C and D rings, with the sole exception of the C-7 ester methyl, which appeared to have significant complexation shifts. These considerations, together with numerous saturation transfer experiments[22] provided a more detailed assignment of the

(22) Mann, B. E. *Prog. Nucl. Magn. Reson. Spectrosc.* **1977**, *11*, 95–114.

Table II. Titration of BChlide-*d* [Et, Et] in $CDCl_3$ with CD_3OD[a]

	mol equivalents of CD_3OD added						plus pure CD_3OD, μL						
resonance	0	0.5	2.00	4.00	8.00	12.00	+2	+4	+6	+8	+10	+12	+20
meso β	9.68	9.67	9.67	9.66	9.65	9.65	9.61	9.58	9.57	9.56	9.55	9.54	9.53
meso α	7.47	7.47	7.51	7.50		7.5	8.05	8.50	8.77	9.04	9.16	9.26	9.35
	6.75	6.75	6.77	8.80									
meso δ	8.36	8.36	8.35	8.30	8.16	8.18	8.16	8.17	8.19	8.21	8.22	8.22	8.23
	7.91	7.91	7.93	8.0									
2a-H									5.29	5.67	5.87	6.02	6.17
10-CH_2	5.33	5.26	5.23	4.93	5.06	5.06	5.09	5.09	5.13	5.15	5.16	5.17	5.18
	4.90	4.90	4.93			4.96	4.96	4.96	5.00	5.02	5.03	5.04	5.06
8-H	4.66	4.64	4.63	4.62	4.62	4.61	4.54	4.50	4.47	4.43	4.44	4.44	4.43
7-H	4.37	4.37	4.39	4.46	4.47	4.44	4.37	4.32	4.30	4.27	4.26	4.25	4.24
5a-CH_2	{3.87–4.15	{3.89–4.14	{3.97	{3.96	{3.93	4.02	4.04	4.00	4.01	4.04	4.02	4.03	4.03
4a-CH_2						3.92	3.85	3.82	3.79	3.77	3.75	3.75	3.76
7d-OMe	3.50, 2.94	3.49, 2.94	3.40, 2.94	3.1–3.5	3.25	3.24	3.23	3.27	3.30	3.35	3.38	3.41	3.45
3-Me	(3.42,	(3.42,	(3.42,					3.23	3.24	3.24	3.25	3.25	3.25
	3.13)	3.12)	3.14)										
1-Me	(1.19,	(1.19,	(1.19,	1.8	1.9	1.8	2.2	2.6	2.77	2.98	3.08	3.16	3.22
	1.92)	1.92)	1.92)										
7b	3.2, 3.4	3.2, 3.4				2.66	2.61	2.58	2.62	2.59	2.55	2.54	2.48
7a	2.8, 2.9	2.8, 2.9				2.3	2.27	2.27	2.24	2.19	2.18	2.19	2.17
2b-Me	0.73	0.73	0.73	0.74	0.75	0.83	1.14	1.43	1.64	obsc	1.9	1.99	2.05
	0.41	0.41	0.43										
5b-Me	{(1.92,	{(1.92,	{(1.92,	{(1.92,	{(1.92,	{(1.92,	{(1.85,	1.86	1.88	1.89	1.90	1.91	1.91
	1.92)	1.92)	1.92)	1.92)	1.92)	1.92)	1.85)						
4b-Me	{(1.42,	{(1.42,	{(1.42,	{(1.42,	{(1.42,	{(1.42,	{(1.42,	1.80	1.77	1.74	1.73	1.72	1.71
	2.04)	2.04)	2.04)	2.04)	2.04)	2.04)	2.04)						
8-Me	(1.68,	(1.68,	(1.68,	(1.68,			1.91	1.86	1.81	1.79	1.77	1.77	1.76
	2.54)	2.54)	2.54)	2.54)									

[a] Initial concentration = 4.7 mM. Initial sample volume 0.5 mL. Chemical shifts to Me_4Si. Assignments in parentheses are tentative.

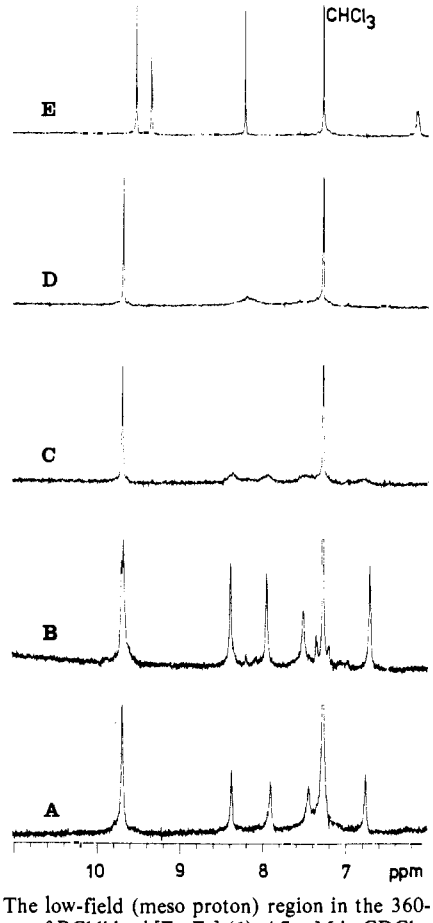

Figure 2. The low-field (meso proton) region in the 360-MHz proton NMR spectra of BChlide-*d* [Et, Et] (**1**), 4.7 mM in $CDCl_3$: (A) at room temperature; (B) at −50 °C; (C) at room temperature with ca. 2 mol equiv of CD_3OD; (E) at room temperature with a large excess of CD_3OD.

dimer spectrum. The saturation transfer experiments were performed with the same technique as for a differential NOE experiment[23] and, indeed, gave both saturation transfer and NOE effects (Figure 1, parts D and E) as even in chloroform solution the line widths of the peaks (ca. 20 Hz half-height width) show that there is still considerable exchange between the dimer molecules. Negative NOE effects, as observed, are not unexpected on the basis of the size of the dimer and the high magnetic field at which the spectra are measured. Figure 1D demonstrates that irradiation of the single methyl peak at 1.2 ppm produces a saturation transfer effect at 1.9 ppm and also a detectable NOE at both of the δ-meso protons. This immediately assigns both methyl signals as C-1 in the dimer. A similar experiment assigning the C-3 methyls by virtue of the NOE to the α-meso protons is shown in Figure 1E.

The saturation transfer experiments were insufficient to provide a complete assignment of the dimer spectrum, particularly of the C-7 ester methyl (C-7*d*) peaks, and these were unambiguously assigned from the spectrum of the d_5-deuterated BChlide-*d*, **2** (Figure 1B). This is of considerable interest as the two ester

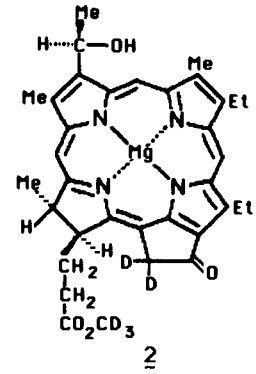

2

methyl signals in the dimer (arrowed in Figure 1A) show very different complexation shifts and line widths. One has a significant upfield complexation shift and is very broad, whereas the other has a very small complexation shift and is sharp. This key experiment enabled the full assignment of the dimer spectrum to be obtained with the only proviso being the pairs of signals due to the C-4b, C-5b, and C-8a methyls. The two methyl signals

(23) Noggle, J.; Schirmer, R. "The Nuclear Overhauser Effect"; Academic Press: New York, 1972.

Table III. Observed and Calculated Complexation Shifts[a] ($\Delta\delta$) for Methyl Bacteriochlorophyllide *d* [Et, Et] (**1**)

proton	obsd shifts	calculated shifts	
		"piggy-back"	face-to-face
meso α	−2.82, −2.10	−2.73, −2.19	−2.76, −2.16
meso β	0.05, 0.05	0.12, 0.12	0.18, 0.18
meso δ	−0.02, −0.49	−0.03, −0.39	−0.14, −0.43
1-Me	−1.37, −2.10	−1.35, −2.26	−1.34, −2.17
3-Me	−0.12, 0.17	−0.31, −0.12	−0.14, 0.02
2b-Me	−1.62, −1.29	−1.70, −1.48	−1.85, −1.79
7d-OMe	−0.06, −0.62	0.09, −0.80	−0.04, −0.80
4a-CH_2	0.19, 0.09	0.19, 0.07	0.25, 0.23
4b-Me	−0.02, 0.84	−0.02, 0.30	0.03, 0.04
5a-CH_2	0.11, −0.03	0.12, 0.08	0.14, 0.13
5b-Me	0.03, 0.03	0.04, 0.15	0.05, 0.05
7-H	0.33, −0.07	0.18, 0.07	0.09, 0.08
8-H	0.12, 0.12	0.05, 0.27	0.36, 0.40
8-Me	0.25, −0.37	0.31, −0.04	0.00, −0.04
10-CH_2	0.22, −0.24	0.07, 0.14	0.17, 0.18
	0.09, −0.10	0.13, 0.07	0.09, 0.09

[a] $\Delta\delta = \delta_{complex} - \delta_{monomer}$.

comprising each pair can be assigned from the saturation transfer experiments, but their unique absolute assignments cannot be made experimentally. (Note that the line widths in the dimer spectrum preclude simple decoupling experiments). The provisional assignments given (Table I) have been made on the basis of the calculated shifts (see later).

Determination of the Dimer Geometry

The experimental complexation shifts ($\delta_{dimer} - \delta_{monomer}$) recorded in Table III may now be used to investigate the structure and conformation of the BChlide-*d* [Et, Et] (**1**) dimer. The unparalleled richness and complexity of the Bchlide-*d* spectrum, giving >30 complexation shifts, make the geometry determination both more sensitive and more critical than our previous structure determinations. Thus, it is important to emphasize the implicit assumptions in this procedure. We have already commented on the accuracy of the ring-current model used and also the convenient simplification of assuming a dimer structure with the chlorophyll planes parallel. A further central assumption is that the complexation shifts are due entirely to the ring-current effects of the neighboring molecule in the dimer. This will only be true if the conformation of each molecule in the dimer is precisely the same as that of the monomer. We shall show that this is certainly not the case for some of the peripheral substituents with attached ligands (e.g., the C-2 and C-7 side chains) for which the conformations differ for the two molecules in the dimer. Thus, in order to define the basic dimer geometry (i.e., the relative position and orientation of the macrocycles) we considered initially for the computational search procedure only those complexation shifts from nuclei rigidly attached to the macrocycle. In view also of possible conformational changes in ring D upon complexation (see later), the basic set used was restricted further to the three meso protons and the β-methyls at C-1 and C-3. This, however, still gives 10 complexation shifts (i.e., equations) in the 4 unknowns defining the dimer geometry, so the search procedure is still overdetermined.

The coordinate system used is shown with the structure of **1**. The base molecule is centered on the origin and lies in the *xy* plane with the α-meso proton along the *y* axis. The second molecule is defined by the coordinates of its center, together with the rotation of the molecule an angle θ about an axis through the magnesium atom parallel to the *z* axis. As the BChlide-*d* molecule is chiral, these four parameters only define the conformation of the dimer for a given type of dimer structure. There are, however, two possible types of dimer structure, a face-to-face structure in which the corresponding faces of the molecule face each other, or a "piggy-back" structure in which both molecules are in the same orientation so that the upper side of one faces the lower side of another. We wish to consider each of these possibilities in turn.

"Piggy-Back" Dimer. The overall pattern of the observed complexation shifts clearly indicates that the second macrocycle is centered around the C-2 1-hydroxyethyl group, and the computational search homed to this position. The displacement coordinates of the top molecule are −2.9, 5.1, and 3.7 Å, with an angle of rotation about the symmetry axis of 169°. The root-mean-square error of the observed vs. calculated complexation shifts (Table III) was 0.13 ppm (R_x 0.10), over a range of values from −2.8 to +0.1 ppm. Even when due consideration is given to possible errors involved in this process, the agreement between the observed and calculated shifts and the consequent definition of the molecule parameters is encouraging. The dimer structure is immediately rationalized as one in which the molecules are joined by coordination of the magnesium atoms to the oxygens of the 2-(1-hydroxyethyl) substituents (Figure 3B). This will be considered further subsequently.

With the basic structure thus defined, the complexation shifts of the mobile side chains can be investigated. The shifts of the two side chains with coordinating groups, i.e., the C-2 and C-7 side chains, are of particular interest as they provide a unique probe into the nature of the coordination sites in the dimer. In both cases it is necessary to consider not only the ring-current shifts at the side-chain protons due to the neighboring BChlide-*d* molecule but also the effect on these protons of the ring current of the parent molecule if the orientation of the side chains in the dimer differs from that in the monomer. This is simpler to evaluate for the 2-(1-hydroxyethyl) side chain; here, the large complexation shifts to the C-2b methyls, resulting in the two signals at 0.4 and 0.7 ppm, were one of the most characteristic features of the dimer spectrum. We shall concentrate on the analysis of these methyl complexation shifts as the assignment of the C-2a proton in the dimer spectrum is only tentative. There is some evidence, from intensity measurements, of a single proton signal at ca. 2.5 ppm (under the C-4b methyl signal) with a NOE to the α-meso proton, and this may be a C-2a proton; the signals of the other C-2a proton and of the two hydroxyl protons have not been identified.

The orientation of the hydroxyethyl substituent in the monomer is not known. In the crystals of methyl bacteriopheophorbide *d* [Et, Et] (**3**) and methyl bacteriopheophorbide *d* [iso-Bu, Et] (**4**)

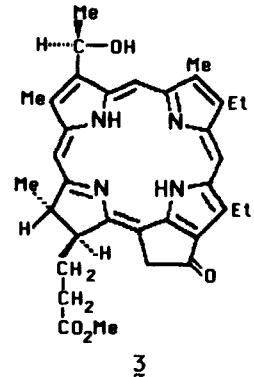

3

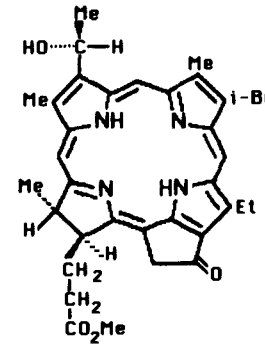

4

the two molecules in the unit cell are joined by hydrogen bonds between the C-2a hydroxyl of one molecule and the C-9 carbonyl of another; in one case a dimer structure results, while in the other a linear polymer is preferred, and these crystal structures are a result of the solvents from which the molecules were crystallized.[24,25] In both these cases the hydroxyethyl substituent has the C-2b methyl almost orthogonal to the chlorophyll plane (dihedral angles ca. 60–90°), which would be anticipated both on steric grounds and also to allow access to the C-2a hydroxyl. In yet a third mode of crystal packing, the hydroxyl of the 2-(1-hydroxyethyl) in methyl bacteriopheophorbide *d* [Et, Et] (**3**) coordinates with the C-7c carbonyl oxygen,[25] setting an interesting precedent (see later).

In the BChlide-*d* dimer proposed here, the C-2a oxygen atoms coordinate with the magnesium atom of the adjacent molecule,

(24) Smith, K. M.; Goff, D. A.; Fajer, J.; Barkigia, K. M. *J. Am. Chem. Soc.* **1983**, *105*, 1674–1676.
(25) Fajer, J.; Barkigia, K. M.; Smith, K. M.; Goff, D. A. manuscript in preparation.

and this coordination will be maximum for a conformation in which the oxygen atom is directly over the magnesium with a dihedral angle to the porphyrin plane (OCCC) of ca. 30–60°. This allows maximum interaction of the oxygen lone pair and the magnesium. The observed ring-current shifts of the C-2b methyls (1.3, 1.6 ppm) will be made up of upfield shifts due to the ring current of the adjacent molecule, which is calculated as ca. 1.6–1.7 ppm, plus a low-field shift from the parent molecule ring current due to any rotation from the orthogonal position of the C-2b methyl. This is calculated to be 0–0.4 ppm for a rotation of 0–45°. The agreement is thus essentially complete, though it is not possible to assign the individual methyl signals to the upper and lower BChlide-*d* molecules from these considerations alone (see later). The calculated complexation shifts for the C-2a proton for the above conformations of the C-2 side chain are ca. 2.8 and 3.1 ppm for the two molecules of the dimer, in fair agreement with the observed shifts from provisional assignments given (3.7 ppm).

The complex pattern produced by the four anisochronous protons of the C-7 CH_2CH_2 side chain has been assigned in the monomer following previous analyses of this system,[1,26] and the C-7b pair has been definitively identified on the basis of base-catalyzed deuteration experiments (Experimental Section) in which the d_6-deuterated BChlide-*d* [Et, Et] **5** was obtained bearing

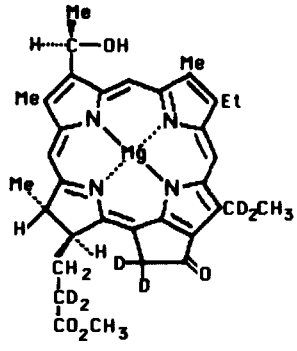

5

deuterium in the C-5a, C-7b, and C-10 methylenes. The spectrum of **5** is shown in Figure 1C. However, only the complexation shifts of the ester methyl protons were used in this investigation. The methyl ester protons are, however, of considerable interest, and they also were identified with the regioselectively d_5-labeled compound **2**. The two methyl signals were very different in appearance, a sharp signal at lower field (complexation shift −0.06 ppm) and a much broader signal at higher field with a large upfield complexation shift of −0.62 ppm. These very contrasting signals may be interpreted in terms of possible conformations of the C-7 side chain. The conformation of this side chain in some monomeric chlorophyll derivatives in solution has been determined by analysis of the vicinal coupling in the C-7/C-7a and C7a/C-7b fragments.[1,26] The favored conformation of methyl pheophorbide *a* and a pheofarnesin derived from BChl-*d* has C-7α, C-7, C-7a, C-7b anti; i.e., θ(7, 7a) = 180°, and C-7, C-7a, C-7b, C-7c anti; i.e., θ(7a, 7b) = 180°.[26] In Chl-*a* the rotamer distribution around the C-7a/C-7b fragment was somewhat less biased toward the favored conformation than in non-magnesiated compounds, and the couplings in the C-7/C-7a fragment could not be extracted from the spectrum.[1] The preferred conformation of the C-7 side chain in solution is that which is found in the crystals of 2-(*S*)-methyl bacteriopheophorbide *d* [iso-Bu, Et];[24,25] thus we may reasonably assume that this conformation is the preferred one for monomeric BChlide-*d* [Et, Et] (**1**) in solution. Finally, the crystal studies show that the ester group has the cis MeOC=O conformation, which is the strongly preferred conformation for all methyl esters.[27]

The complexation shifts of the ester methyl protons in the dimer *on the basis of the above side-chain conformation* may be calculated directly to give values of 0.09 and 0.05 ppm respectively for the upper and lower molecules. Clearly, these values are in agreement with only *one* of the observed complexation shifts, the large upfield shift of the broad signal, is not reproduced on this basis. The clear inference is that one of the C-7 side chains adopts a different conformation upon formation of the BChlide-*d* dimer. It is not difficult to identify which side chain this will be; in the

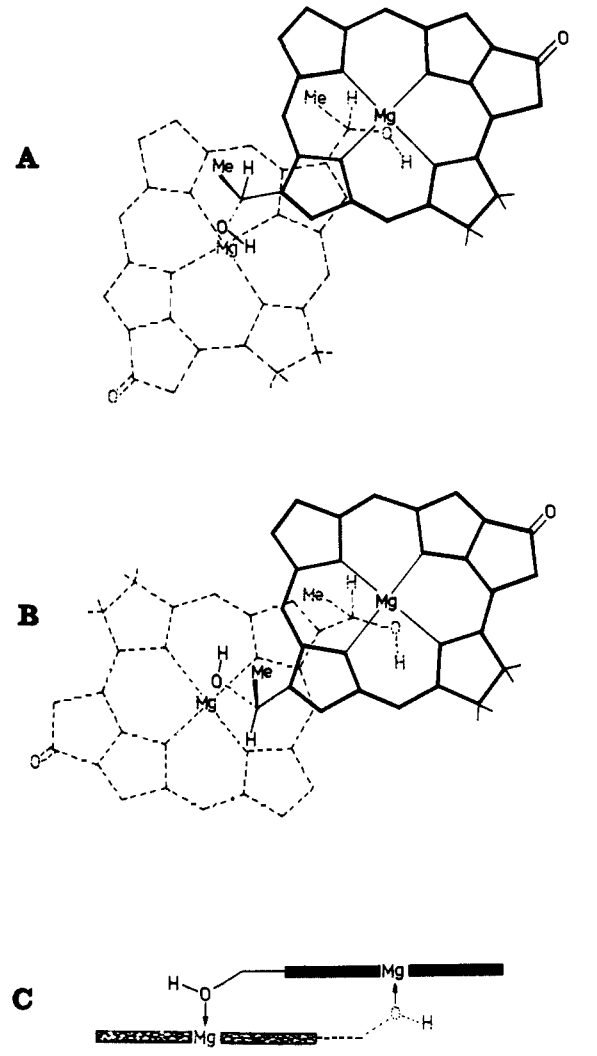

Figure 3. Proposed dimer structure of BChlide-*d* [Et, Et] (**1**): (A) face-to-face; (B) "piggy-back"; (C) end-on projection.

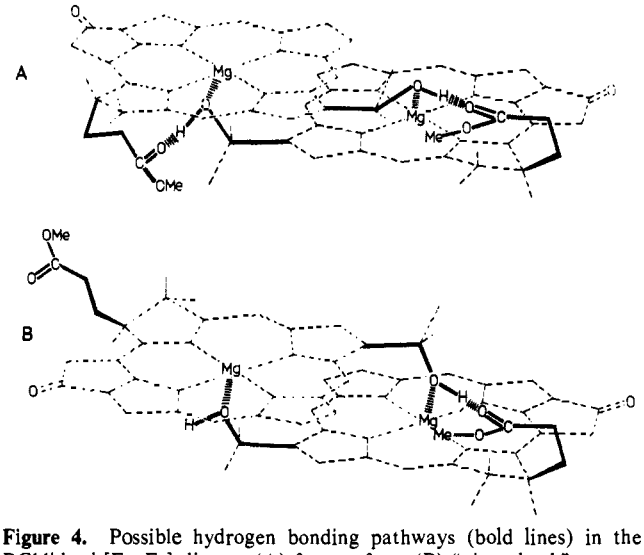

Figure 4. Possible hydrogen bonding pathways (bold lines) in the BChlide-*d* [Et, Et] dimer: (A) face-to-face; (B) "piggy-back".

(26) Smith, K. M.; Goff, D. A.; Abraham, R. J. *Tetrahedron Lett.* **1981**, *22*, 4873–4876.
(27) Jones, G. I. L.; Owen, N. L. *J. Mol. Struct.* **1973**, *18*, 1–32.

"piggy-back" dimer considered (Figures 3B and 4B) the C-7 side chain on the upper molecule is on the opposite face of the molecule from the coordination site and will presumably be free to adopt the same conformation in solution as the monomer. The sharp low-field methyl signal is then assigned to the methyl of this side chain, in accord with the calculated shifts. The other C-7 side chain is on the same side of the molecule as the site of coordination. Molecular models show that, in the "normal" conformation of this side chain, the dimer geometry is such that there are no repulsive steric interactions with the adjacent molecule and that this is a quite reasonable conformation. However, further detailed inspection of the dimer geometry shows that when the C-2a oxygen atom in the upper molecule coordinates with the magnesium of the lower one, the hydroxyl proton could be pointing directly toward the γ-meso position; conditions are now ideally set up for an intermolecular hydrogen bond between the C-7c carbonyl of the lower molecule and the hydroxyl of the upper molecule, but now the conformation of the C-7 side chain is folded back over the parent molecule (as illustrated in Figure 4B). This C-7c carbonyl interaction with the 2-(1-hydroxyethyl) hydroxyl is also in accord with observations in the X-ray structure of methyl bacteriopheophorbide *d*.[24,25] The complexation shift of the ester methyl protons (C-7d) in this conformation is made up of contributions from the ring currents of both BChlide-*d* molecules; these are calculated as −0.90 ppm from the lower molecule and +0.10 ppm from the upper to give an overall complexation shift of −0.80 ppm, which is in satisfactory agreement with the observed value of −0.62 ppm. The implications of this geometry will be considered subsequently, but it does provide a simple rationale for the assignment of the C-2b methyl signals. The methyl of the hydrogen-bonded hydroxyethyl substituent would be expected to experience a downfield shift due to the proximity of the ester carbonyl group and is therefore assigned to the 0.74 ppm signal.

The remaining substituent groups can now be considered. The C-4 and C-5 ethyl substituents would be expected to prefer an orthogonal orientation with respect to the molecular plane to minimize steric repulsions with the adjacent substituents. In the proposed dimer structure the C-5 substituent is well removed from any interaction with the neighboring molecule and should not be affected by the complexation. In support of this the observed complexation shifts of the methyl and methylene protons are in good agreement with those calculated for an orthogonal conformation. Similar calculations for the C-4 ethyl group give excellent agreement with the observed complexation shifts for all the methyl and methylene signals except that a significant low-field shift of one methyl substituent is not well reproduced in the calculations. The C-4 substituent is reasonably close to the substituents in the adjacent molecule in the proposed dimer structure and may experience some displacement from the orthogonal orientation, which would give an additional low-field shift. However, as the C-4b and C-5b methyl signals are not definitively assigned, it is not profitable to consider them in more detail at this stage.

The complexation shifts of the remaining C-7 and C-8 substituents, i.e., C-7H, C-8H, and C-8 Me, will be dependent upon the conformation of ring D. Crystal structure studies have shown that this ring can adopt several different conformations. In ethyl Chlide-*a* an envelope conformation was observed[28] in which C-8 is in the molecular plane and C-7 is displaced above the plane by ca. 0.3 Å; conversely, in methyl bacteriopheophorbide *d* [Et, Et] a half-chair conformation is found in which C-8 is above and C-7 below the molecular plane by ca. 0.3 Å, while in methyl bacteriopheophorbide *d* [neo-Pn, Et] ring D is almost planar.[24,25] These different conformations can be rationalized in terms of the various hydrogen bonding networks and other packing forces found in the crystals. From this it is quite likely that the conformation of ring D in the dimer will differ from that in the monomer, and also due to the differing bonding requirements of the C-7 substituents in the two molecules, it is probable that the conformation will be different for the two molecules of the dimer. The complexation shifts for these protons have been calculated on the basis of a planar conformation for ring D. There is generally reasonable agreement with the observed shifts (Table III), which is all that could be expected without more detailed knowledge of the dimer geometry.

The Face-to-Face Dimer. We may now consider, using the same procedure as above, the other possible dimer structure, namely the face-to-face dimer. Whereas there is only one type of dimer for the "piggy-back" model, there are two possible types of dimer for the face-to-face model, depending on which face of the BChlide-*d* molecule is exterior and which is interior. These two structures will of course give the same agreement in the basic search procedure as only nuclei in the molecular plane are used (i.e., the meso protons and the C-1 and C-3 methyls). The differences are only apparent when the side-chain complexation shifts are considered.

The computational search using the meso and β-methyl protons and the face-to-face model gave displacement coordinates −3.4, 4.3, 3.2 Å, with an angle of rotation about the symmetry axis of −71°. The root-mean-square error of the calculated vs. observed shifts was 0.09 ppm (R_x 0.068), i.e., in essentially complete agreement. The structure is again one in which the hydroxyl atoms of the C-2 1-hydroxyethyl substituent are coordinated with the magnesium atom of the adjacent molecule. In this dimer structure both the C-7 side chains are internal, that is, oriented toward the adjacent molecule (Figures 3A and 4A). The alternative dimer structure simply has the opposite displacement along the z axis; i.e., the displacement coordinates are identical, but with $z = -3.2$ Å. In this structure the C-7 substituents are oriented away from the adjacent molecule. This immediately provides a differentiation between the two face-to-face structures as in the alternative structure the C-7 substituents would be incapable of any interaction with the adjacent molecule. Thus it is not possible on the basis of this alternative structure to give any reasonable explanation for the C-7d methyl complexation shifts, and we shall not consider this any further.

The complexation shifts of the side-chain protons may now be considered on the basis of the face-to-face structure in Figure 3A, in exactly the same manner as for the "piggy-back" model, but again the qualifications to this procedure previously discussed still apply. The C-2b methyl complexation shifts are calculated to be −1.85 and −1.79 ppm for an orthogonal orientation of the methyl groups. This is the optimum orientation for Mg···O interactions, and also any rotation from this position produces larger complexation shifts in disagreement with observation. The C-7d methyl ester complexation shifts can be calculated in precisely the same manner as for the "piggy-back" dimer. It is possible to envisage in this structure also a hydrogen bond between the C-2b hydroxyl and the C-7c carbonyl group of a folded back C-7 side chain (Figure 4A). In this conformation the complexation shifts of the C-7 ester methyl are identical with those given above for the "piggy-back" dimer as the major contribution to the shifts is from the parent molecule in both cases. However, what is not clear on this structure is why only one C-7 substituent behaves in this fashion because the structure would appear to allow for both C-7 substituents to interact in this way (Figure 4A, see later).

The remaining side-chain complexation shifts were calculated in the same manner as for the "piggy-back" dimer and are given in Table III. There is overall agreement with the observed shifts, but with certain exceptions. The large low-field shift of one of the C-4b methyls is not well reproduced as are the calculated shifts for the C-8 methyl. Note that although the face-to-face structure does not have twofold symmetry, i.e., the two molecules are not identical, there is more similarity between the two molecules in the dimer, especially with regard to the side chains, than in the "piggy-back" model. Thus, the differences between the complexation shifts of any one substituent are less easy to explain on this model.

Optical Spectra of the Dimer

Electronic absorption spectra of the dimer in $CDCl_3$ under conditions identical with those used for the NMR spectra showed

(28) Chow, H. C.; Serlin, R.; Strouse, C. E. *J. Am. Chem. Soc.*, **1975**, *97*, 7230–7237.

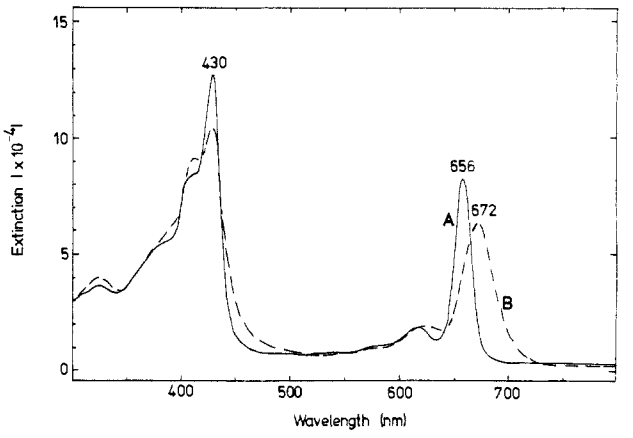

Figure 5. Electronic absorption spectra of BChlide-*d* [Et, Et] (**1**): (A) in $CDCl_3$ containing pyridine; (B) in pure $CDCl_3$.

a clear red shift from that of the monomer (produced by addition of pyridine to the dimer spectrum), Figure 5. These spectra clearly indicate, on the basis of the red shift of 16 nm, that some kind of aggregation is taking place. We have previously measured the electronic absorption of BChls-*d* in hexane, and in this case a more extensive red shift of 72 nm was observed, the hexane species being interpreted (on the basis of its similarity with the spectrum of the antenna array in living cells) to be derived from an aggregate of 13-14 BChl-*d* molecules.[13] Thus, the optical spectra clearly indicate an aggregate of considerably smaller size than one containing 13–14 molecules, and they are entirely consistent with the proposed dimer structure.

Energy of Formation of the Dimer

In view of the exceptional stability of the BChlide-*d* dimer, it is of interest to consider whether the NMR data can provide any estimate of the energy of formation of the dimer. In pure chloroform solution at room temperature the half-height width of a single resonance in the BChlide-*d* dimer is ca. 12 Hz, as compared with the comparable line width in the monomer spectrum of 1–2 Hz (cf. Figure 1). If this increase in line width can be attributed solely to exchange between the different sites in the dimer, presumbly via dissociation and recombination, as in eq 1, then the

$$B_2 \underset{k_c}{\overset{k_d}{\rightleftharpoons}} 2B \qquad (1)$$

dissociation rate constant k_d is obtained from this line broadening by the rate equation 2 for the slow exchange limit.[29]

$$k_d = 2/\tau = 2\pi(\Delta\nu - \Delta\nu_0) \qquad (2)$$

The factor of 2 arises because the monomer molecules can recombine to give the same dimer as before, with equal probability to the exchange mechanism. The value of k_d obtained (60 s^{-1}) is an upper limit as any other contribution to the dimer line width, such as decreased relaxation time compared with the monomer, etc., will decrease the value of k_d. The lower limit of k_d may be obtained from the saturation transfer experiments. The condition for complete saturation transfer, which is observed in our experiments, is that the exchange rate is much less than the relaxation rate $(1/T_1)$.[30] The proton relaxation time in such large molecules is of the order of 0.1 s,[29] giving a lower limit for the exchange rate of 10 s^{-1} and therefore of k_d of 20 s^{-1}.

An order of magnitude value of the recombination rate (k_c) of the monomeric BChlide-*d* molecules is the diffusion-controlled limit, which in chloroform at 25 °C is 12.1 × 10^9 L mol^{-1} s^{-1}.[31] These values provide an estimate for the equilibrium constant for eq 1 of 5 × 10^{-9} mol L^{-1}, which corresponds to the dissociation free energy of the dimer of 11.5 kcal mol^{-1}. An independent estimate of the dissociation energy may be obtained from the observation that even in the most dilute solutions examined (<1 mM) no evidence of monomer formation was apparent. Assuming that 5% of the monomer could be detected under these conditions, which is certainly an upper limit, simple kinetics based on eq 1 give a value of the equilibrium constant (K; eq 1) of $<10^{-6}$ mol L^{-1}, i.e., $\Delta G > 8$ kcal mol^{-1}. Thus, the available evidence is consistent with a value of the dissociation energy of the dimer considerably larger than 8 kcal mol^{-1} and ca. 11 kcal mol^{-1}.

Comparable analysis of the coalescence phenomena occurring in the NMR spectrum upon addition of ligands (L) such as methanol, can be shown to be consistent with reactions such as those in eq 3 and 4.

$$B_2 + L \rightleftharpoons BL + B \qquad (3)$$

$$B + L \rightleftharpoons BL \qquad (4)$$

However, it was not considered feasible to undertake a more detailed full lineshape analysis based on these equations in view of the complex nature of the system and the spectra involved.

Discussion

In the preceding section it was shown that two dimer structures are compatible with the observed complexation shifts, and it is not possible simply on the basis of the calculated shifts alone to unambiguously decide on the preferred model. The basic search procedure gives somewhat better agreement for the face-to-face model, but the complexation shifts of the side-chain protons are more easily explained on the "piggy-back" model. These two alternative structures can only be differentiated on the basis of more general considerations. These are given particular interest by the very recent X-ray structure analysis of a membrane protein complex containing the photoreaction center from the purple bacterium *Rhodopseudomonas viridis*.[32] In this complex, two bacteriochlorophyll *b* molecules form a "closely associated, noncovalently linked dimer (special pair)". The arrangement of this dimer structure is of the face-to-face type with ring A in one molecule overlapping ring A of the neighbor, but, however, the C-7 propionic side chains are facing outward from the coordination site, which involes the C-2a acetyl carbonyl oxygen and the magnesium of the neighboring molecule.

The calculations indicate an average separation between the parallel macrocyclic ring planes of about 3.5 Å, and Mg···O distances (with the magnesium atom to be in the ring plane) of approximately 2.6 Å; if one assumes, with good justification, that the magnesium is pulled approximately 0.4–0.5 Å out of the macrocyclic ring plane by the coordinating ligand, this would afford a Mg···O distance of about 2.1–2.2 Å, well in accord with the X-ray observations of Chow et al.[28]

Considering again the complex formed in solution, there are two contrasting phenomena that any model needs to explain. One is the considerable stability of the complex in solution, while the other is the relative absence, certainly compared with the analogous Chl-*a* and -*b* complexes in solution,[11a] of any oligomeric species. All the available evidence is consistent with the formation of a stable BChlide-*d* dimer in chloroform solution. The spectrum is unchanged over the entire concentration range studied (which was not great, <1 mM to ca. 5 mM, the red-shifted optical spectra were unchanged over the range 40 μM to 4 mM); the complex also appears to be present to some extent even in strongly polar solvents such as acetone-d_6, and a large molar excess of complexing ligands is necessary to disaggregate the dimer. In this respect water behaves exactly the same as methanol, but the dissociation of the BChlide*d* dimer with added D_2O cannot be driven to completion because of the limited solubility of D_2O in chloroform. This again illustrates the difference between this dimer and the Chl-*a* aggregates, where a molecule of water is implicated in the aggregate structure.[11]

(29) Abraham, R. J.; Loftus, P. "Proton and Carbon-13 NMR Spectroscopy"; Wiley-Heyden: London, 1981; p 168.
(30) Martin, M. M.; Martin, G. J.; Delpuech, J. J. "Practical NMR Spectroscopy"; Wiley-Heyden: London, 1980; p 317.
(31) Wilkinson, F. "Chemical Kinetics and Reaction Mechanisms"; van Nostrand-Reinhold Co.: New York, 1980; p 139.
(32) Deisenhofer, J.; Epp, O.; Miki, K.; Huber, R.; Michel, H. *J. Mol. Biol.* **1984**, *180*, 385.

There is, however, no evidence in the chloroform solutions examined of any oligomeric solutions, in contrast to the large oligomers present even in dilute solutions of Chl-*a* and -*b* in chloroform. In very nonpolar solvents such as hexane the electronic absorption spectra of BChl-*c*, -*d*, and -*e* show pronounced red shifts which are considered to be due to formation of large aggregates;[13] unfortunately, the solubility of BChl-*d* in hexane is too low to obtain any NMR spectrum. Thus, the evidence points to a specific stable dimer structure in which the formation of higher aggregates, trimers, tetramers, etc., is a different, higher energy process. This would appear to favor the face-to-face structure as in this structure the addition of a further molecule of BChlide-*d* to form a trimer must involve a different type of interaction from that present in the dimer. In the "piggy-back" dimer it is conceptually easier to envisage the formation of an oligomeric species. However, further consideration shows that these geometrical factors may not be essential. In the dimer there are two Mg···O coordination links; this is supported both by the geometries and by the estimated dissociation energy of ca. 11 kcal mol^{-1}, corresponding to the breaking of two Mg···O bonds.[33] As in all chlorophyll chemistry, the magnesium is never more than five coordinate to attached oxygen ligands,[4] in the trimer there can only be two Mg···O bonds, and in the *n*-mer, $n - 1$ Mg···O bonds. Thus, the dimer is intrinsically more stable than any oligomer, possessing one Mg···O coordination link per monomer unit.

This essentially thermodynamic argument is, of course, independent of the precise structure of the dimer provided only that there are two Mg···O coordinating bonds; thus, it applies equally to all the structures considered. The differentiation between the possible models of the solution complex hinges basically on the observed complexation shifts of the side chains and in particular of the C-7 propionate ester. The strikingly different behavior of the two ester methyls upon dimer formation, in which one methyl appears to be in the neighborhood of the coordination site (as evidenced by the sizeable upfield complexation shift) and the other is essentially unchanged from the monomer, has a simple and obvious rationale on the basis of the "piggy-back" model (Figure 4B). Here the environment of the two C-7 side chains is by definition quite different, one being endo and one exo to the dimer architecture. In contrast there is not such an obvious explanation of this phenomenon on the basis of the face-to-face models. In the structure shown in Figure 4A, in which both the C-7 side chains are endo, it is possible to imagine that one propionate ester group could hydrogen bond to the coordinating C-2a hydroxyl and not the other, as the complex does not have twofold symmetry. This does not appear very likely. In the structure analogous to that found in the "special pair" dimer[32] the C-7 side chains, which bear large fatty esterifying alcohols, are both exo to the dimer complex and there is no good reason for any interaction with the coordination site. In agreement with this, the X-ray structure shows two extended C-7 side chains pointing away from the macrocycles.

Another argument in favor of the "piggy-back" model is the slow rate of interchange of the two molecules in the dimer. In the preceding section it was shown to be consistent with a dissociative mechanism with a large activation energy. This is necessary for the "piggy-back" model as the molecules cannot interchange without dissociating. However, the face-to-face model could exchange sites in the NMR spectrum *without* dissociating; a lateral movement of the BChlide-*d* molecules with respect to each other could interconvert the molecular sites. Intuitively, this would be expected to be a much lower energy process than the observed one. Intriguingly, the special pair dimer structure of the crystal analysis is to all intents and purposes of twofold symmetry; i.e., the two molecules of the dimer are equivalent by symmetry.[32] Thus, a structure of this type is incompatible with all of the BChlide-*d* NMR observations.

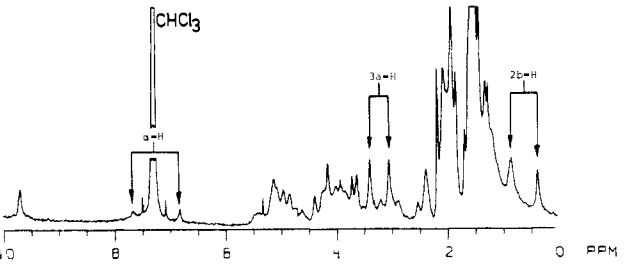

Figure 6. 500-MHz NMR spectrum of the BChls-*c* (**6**),[36] 3 mM in $CDCl_3$.

Extension to the Bacteriochlorophyll *c* Series. Since the BChl-*c* (**6**)[36] also possess the functional features required for dimer

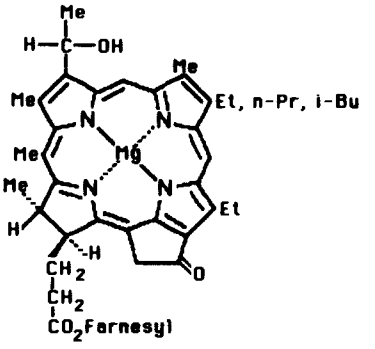

6

formation, our study was extended to include these compounds. The complete mixture of BChl-*c* homologues (containing >70% of the [Et, Et] homologue) was dissolved in $CDCl_3$, and the spectrum obtained under conditions described earlier is shown in Figure 6. The BChl-*c* clearly form a dimer that is very similar to that for BChlide-*d* [Et, Et]; notably, the BChls-*c* possess only two meso protons, the δ-position being occupied by a methyl group.[36] A complete NOE and saturation transfer sequence of experiments were not carried out because of the similarity of the spectra shown in Figures 1A and 6, but those performed are annotated on Figure 6 and clearly demonstrate the similarity between the two BChl systems.

Conclusions

The conclusion reached is that the "piggy-back" model (Figures 3B and 4B) best satisfies the available NMR data for the BChlide-*d* [Et, Et] (**1**) dimer structure in solution. This conclusion must be qualified without more conclusive experimental evidence. An unambiguous assignment of all the peripheral proton resonances would be of interest, as would further spectroscopic investigation into the precise coordination mechanism of the dimer and an X-ray structure of BChlide-*d* crystallized from chloroform. The different structures of the complexes found in solution and in the "special pair" X-ray are particularly intriguing. However, it would be idle to speculate further without more detailed knowledge of the solution complex and perhaps a more refined crystal structure. For example, it is not clear whether 3 Å resolution is sufficient to distinguish two nonidentical BChl-*b* molecules in the "special pair".

Experimental Section

BChlide-*d* [Et, Et] (**1**) was obtained by magnesiation[34] of methyl bacteriopheophorbide *d* [Et, Et], obtained from *Chlorobium vibrioforme thiosulfatophilum* as described elsewhere.[35] It was recrystallized from dichloromethane–hexane and then dried overnight under vacuum at 78 °C. Deuteriochloroform was dried over CaH_2 and then distilled immediately before use. Proton NMR spectra showed no impurities to be present and were recorded either on a Nicolet NT-500 (500 MHz) or a Nicolet NT-360 (360 MHz) spectrometer. Typical conditions were probe

(33) Miller, J. R.; Dorough, G. D. *J. Am. Chem. Soc.* **1952**, *74*, 3977–3981.
(34) Zass, E.; Isenring, H.; Etter, R.; Eschenmoser, A. *Helv. Chim. Acta*, **1980**, *63*, 1048–1067.
(35) Smith, K. M.; Goff, D. A. *J. Chem. Soc., Perkin Trans 1* **1985**, 1099–1115.
(36) Smith, K. M.; Craig, G. W.; Kehres, L. A.; Pfennig, N. *J. Chromatogr.* **1983**, *281*, 209–223.

temperature 23 °C, 16 or 32K data points, sweep width 4 kHz giving a digitization accuracy of 0.25 or 0.5 Hz/point, pulse width 7 Ms, aquisition time 1 or 2 s, and ca. 80 accumulations. Probe temperatures were controlled with the spectrometer variable-temperature control unit, and a 15 min equilibration time was allowed between each spectrum. Saturation transfer experiments were performed by narrowing down the sweep width of, e.g., the Nicolet NT-360 instrument to ±-2000 Hz and then obtaining a 32K spectrum with resolution of 0.3 Hz. The decoupler was set to a chosen frequency at the downfield end of the spectrum (reference) and the second frequency was set to saturate the peak of interest in the BChlide-*d* [Et, Et] dimer. The pulse width was set to zero (hetero mode) and the output level was 28 dB. A decay of about 4 times the aquisition time preceded a 45° pulse (6.00 μs) which was short enought to allow detection of the saturation transfer effects while still observing NOE effects. The decoupler was off during the acquisition time. Fourier transformation followed by subtraction of the saturation transfer spectrum from the reference spectrum gave the difference spectra shown in Figure 1.

Trideuteriomethyl 10,10-Dideuteriobacteriochlorophyllide *d* [Et, Et] (2). A solution of methyl bacteriopheophorbide *d* [Et, Et][35] (33.8 mg) in 3% D_2SO_4/CD_3OD (5 mL) was stirred overnight under a nitrogen atmosphere. Dichloromethane and aqueous sodium acetate were added, and the organic phase was rinsed with water, dried (Na_2SO_4), and evaporated to give a green residue that was chromatographed on a Harrison Research chromatotron, silica gel plate, elution with 3% tetrahydrofuran in dichloromethane. The eluates containing the major green band were evaporated to give a green residue. NMR, (Nicolet NT-500, $CDCl_3$), 9.53 (s, 1 H, α-meso-H), 9.43 (s, 1 H, β-meso-H), 8.45 (s, 1 H, δ-meso-H), 6.26 (q, 2a-H), 5.13 (ABq, 10-CH_2, >95% deuterated), 4.41 (m, 1 H, 8-H), 4.19 (m, 1 H, 7-H), 4.02 (ABX$_3$, 2 H, 5a-CH_2), 3.62 (s, OMe, >95% deuterated), 3.33 (s, 3 H, 1-Me), 3.19 (s, 3 H, 3-Me), 2.50-2.63 and 2.20-2.27 (each m, 5 H, 7a,b-CH_2CH_2 and 2a-OH), 2.06 (d, J = 6.6 Hz, 3 H, 2b-Me), 1.92 (t, J = 7.5 Hz, 3 H, 5b-Me), 1.75 (d, J = 7.2 Hz, 3 H, (-Me), 1.67 (t, J = 7.6 Hz, 3 H, 4b-Me), 0.28, -1.84 ppm (each br s, each 1 H, NH). Magnesium was inserted into this sample with the Eschenmoser BHT procedure[34] to give 16.57 mg (47%) of the required d_5-deuterated BChlide-*d*.

Methyl 5a,5a,7b,7b,10,10-Hexadeuteriobacteriochlorophyllide *d* [Et, Et] (5). A solution of methyl bacteriopheophorbide *d* [Et, Et] (23.9 mg) in CH_3OD (5 mL) containing sodium hydroxide (150 mg) was refluxed for 3 h under a nitrogen atomosphere. The solution was cooled by using an ice/water bath before addition of 25% aqueous acetic acid to pH 7. The mixture was partitioned between dichloromethane and water and washed with aqueous sodium bicarbonate, and the organic phase was dried (Na_2SO_4) and evaporated to give a residue that was redissolved in 3% H_2SO_4 in methanol and stirred for 3 h at room temperature. Dichloromethane and aqueous sodium acetate were added and the organic phase was rinsed with water, dried (Na_2SO_4), and evaporated to give a green residue that was chromatographed on a silica gel preparative plate (elution with 3% tetrahydrofuran in dichloromethane). Extraction of the appropriate band followed by evaporation gave the hexadeuterated methyl bacteriopheophorbide *d* (1.61 mg; 6.8%). NMR, (Nicolet NT-500, $CDCl_3$) 9.53 (s, 1 H, α-meso-H), 9.43 (s, 1 H, β-meso-H), 8.45 (s, 1 H, δ-meso-H), 6.26 (q, 2a-H), 5.13 (ABq, 10-CH_2, ca. 70% deuterated), 4.41 (m, 1 H, 8-H), 4.19 (m, 1 H, 7-H), 4.02 (ABX$_3$, 5-CH_2, >95% deuterated), 3.62 (s, 3 H, OMe), 3.33 (s, 3 H, 1-Me), 3.19 (s, 3 H, 3-Me), 2.65 and 2.29 (each m, each 1 H, 7a-CH_2CD_2), 2.59 (s, 1 H, 2a-OH), 2.06 (d, J = 6.6 Hz, 3 H, 2b-Me), 1.92 (s, 3 H, 5b-CD_2CH_3, 1.75 (d, J = 7.2 Hz, 3 H, -Me), 1.67 (t, J = 7.6 Hz, 3H, 4b-Me), 0.28, -1.84 ppm (each br s, each 1 H, NH). Magnesium was inserted into this sample by using the Eschenmoser BHT procedure[34] to afford the required d_6-deuterated BChlide-*d*.

Acknowledgment. This research was supported by grants from the National Science Foudnation (No. CHE-81-20891) and the Scientific Affairs Division of NATO (No. RG 256.80). We also acknowledge the use of computing facilities at the University of Liverpool and the University of California, Davis and helpful discussions with Dr. R. F. Hout (Stuart Pharmaceuticals, Ltd.).

Gas-Phase Reactions of V^+ and VO^+ with Hydrocarbons Using Fourier Transform Mass Spectrometry

T. C. Jackson,† T. J. Carlin,‡ and B. S. Freiser*

Contribution from the Department of Chemistry, Purdue University, West Lafayette, Indiana 47907. *Received June 17, 1985*

Abstract: The reactions of V^+ and VO^+ with small alkanes are reported. V^+ reacts with hydrocarbons primarily by inducing dehydrogenation, showing a marked preference for C-H bond insertion, giving rise to products corresponding to C-C bond insertion only when C-H reaction pathways are blocked. Unlike later transition metals, V^+ will undergo secondary reactions with most alkanes, producing complexes having more than one hydrocarbon ligand. The presence of oxygen as a ligand on V^+ has surprisingly little effect on reactivity and only influences reactions when coordinative saturation becomes a factor. In contrast to FeO^+, the oxide ligand is not observed to participate in the reactions, due undoubtedly to the strong V^+-O bond.

The study of the chemistry of gas-phase metal ions often begins with an examination of their interactions with hydrocarbons, due to the importance of hydrocarbons in organometallic chemistry and catalysis and also to the ubiquitous presence of a hydrocarbon chain in other organic molecules of interest.[1] Most of the work to date has been concentrated on the groups 8-10 metal cations, Fe^+, Co^+, and Ni^+ due to their importance in catalysis,[2] although preliminary studies have also been reported for a variety of other gas-phase metal ions.[1b,3] This paper is a continuation of our work in this area and reports the reactivity of the early first-row transition-metal ion, V^+, with hydrocarbons. Since oxide chemistry is prominent in the solution chemistry of vanadium, and since formation of VO^+ is observed in the gas-phase reactions of V^+ with many oxygen-containing species, the chemistry of VO^+ is also reported. In a similar study comparing the reactions of Fe^+

† Present Address: Research Laboratories, Eastman Kodak Co., Rochester, NY 14650.

‡ Present Address: Mobile Research and Development Research Laboratory, Paulsboro, NJ 08066.

(1) (a) Allison, J.; Freas, R. B.; Ridge, D. P. *J. Am. Chem. Soc.* **1979**, *101*, 1332. (b) Byrd, G. D.; Burnier, R. C.; Freiser, B. S. *J. Am. Chem. Soc.* **1982**, *104*, 3565. (c) Halle, L. F.; Armentrout, P. B.; Beauchamp, J. L. *Organometallics* **1982**, *1*, 963.

(2) (a) Davidson, P. J.; Lappert, M. F.; Pearce, R. *Chem. Rev.* **1976**, *76*, 219. (b) Jacobson, D. B.; Freiser, B. S. *J. Am. Chem. Soc.* **1983**, *105*, 5197. (c) Jacobson, D. B. Ph.D. Thesis, Purdue University, 1984. (d) Allison, J.; Ridge, D. P. *J. Organomet. Chem.* **1975**, *99*, C11. (e) Corderman, R. R.; Beauchamp, J. L. *J. Am. Chem. Soc.* **1976**, *98*, 5700. (f) Armentrout, P. B.; Halle, L. F.; Beauchamp, J. L. *J. Am. Chem. Soc.* **1981**, *103*, 6624.

(3) (a) Burnier, R. C.; Carlin, T. J.; Reents, W. D., Jr.; Cody, R. B.; Lengel, R. K.; Freiser, B. S. *J. Am. Chem. Soc.* **1979**, *101*, 7127. (b) Weil, D. A.; Wilkins, C. L. *J. Am. Chem. Soc.* **1985**, *107*, 7316. (c) Byrd, G. D.; Freiser, B. S. *J. Am. Chem. Soc.* **1982**, *104*, 5944. (d) Aristov, N.; Armentrout, P. B. *J. Am. Chem. Soc.* **1984**, *106*, 4065. (e) Mandich, M. L.; Halle, L. F.; Beauchamp, J. L. *J. Am. Chem. Soc.* **1984**, *106*, 4403. (f) Tolbert, M. A.; Beauchamp, J. L. *J. Am. Chem. Soc.* **1984**, *106*, 8117.

0002-7863/86/1508-1120$01.50/0